

# Vibrational relaxation in $I_2^-(Ar)_n$ ( $n=1,2,6,9$ ) and $I_2^-(CO_2)_n$ ( $n=1,4,5$ ) clusters excited by femtosecond stimulated emission pumping

Alison V. Davis, Roland Wester,<sup>a)</sup> Arthur E. Bragg, and Daniel M. Neumark<sup>b)</sup>

Department of Chemistry, University of California, Berkeley, California 94720 and Chemical Sciences Division, Lawrence Berkeley National Laboratory, Berkeley, California 94720

(Received 22 January 2003; accepted 1 May 2003)

Vibrational relaxation dynamics in  $I_2^-(Ar)_n$  ( $n=1,2,6,9$ ) and  $I_2^-(CO_2)_n$  ( $n=1,4,5$ ) clusters are studied using femtosecond stimulated emission pumping (fs-SEP) in conjunction with femtosecond photoelectron spectroscopy. fs-SEP generates coherently excited  $I_2^-$  within the cluster; results are reported here for excitation energies of 0.57 and 0.75 eV. The time-dependent PE spectra track relaxation of the clustered  $I_2^-$  through coherent intensity oscillations observed at short times ( $<10$  ps) and shifts of the photoelectron spectra that can be seen out to several hundred picoseconds. The relaxation rates depend on the cluster type and excitation energy: the overall time scale in  $I_2^-(CO_2)_n$  clusters is relatively independent of both, but in  $I_2^-(Ar)_n$  clusters the time scale generally increases with cluster size and decreases with excitation energy. The observed dynamics for  $I_2^-(CO_2)_n$  and several of the  $I_2^-(Ar)_n$  clusters directly probe the time scale for solvent evaporation. © 2003 American Institute of Physics. [DOI: 10.1063/1.1585029]

## I. INTRODUCTION

Small anion clusters comprising an anion chromophore and one or more solvent species have become model systems for studying the influence of molecular solvation on fundamental molecular processes.<sup>1–3</sup> Anions are mass-selectable, allowing the evolution of solvent-dependent dynamics to be examined as a function of the number of solvent species. In addition, the charged chromophore results in relatively strong interactions with the solvent, so that processes such as solvent-induced recombination and vibrational relaxation following photodissociation of the anion chromophore are seen with relatively few solvent atoms/molecules. As a result, cluster studies have provided many points of comparison with condensed-phase studies of dynamics in solution.<sup>4</sup> One of the major research directions in our group and others has been to follow the dynamics that occur upon photodissociation of  $I_2^-$  embedded in a small solvent cluster; such dynamics can become quite complex, especially in larger clusters, where pure dissociation is supplanted by solvent-induced curve-crossing, recombination, and vibrational energy loss on the ground state, with solvent evaporation occurring at any of these stages.

The photodissociation of  $I_2^-$  within argon and  $CO_2$  clusters was first studied by Lineberger and co-workers,<sup>5–8</sup> who measured product distributions and performed time-resolved absorption recovery experiments. In our group, we have used femtosecond photoelectron spectroscopy (FPES)<sup>9–12</sup> to investigate the same processes. This experimental work is complemented by molecular dynamics simulations by Parson and co-workers<sup>2,13–18</sup> and others.<sup>19–22</sup> The two solvent species create very different dynamics. In  $I_2^-(CO_2)_n$  clusters,

recombination on the ground state and vibrational relaxation occur very rapidly. For  $I_2^-(CO_2)_{16}$ , in which the  $I_2^-$  is surrounded by a full solvent shell, recovery of 790 nm absorption occurs with a time scale of only 1.3 ps;<sup>7</sup> simulations of its FPE spectra showed that on this time scale, both recombination and vibrational energy loss occurred, but that complete solvent evaporation took hundreds of picoseconds.<sup>12</sup> In  $I_2^-(Ar)_n$  clusters, time scales for curve-crossing and energy loss are much longer, but evaporation of solvent atoms from the ground state more closely tracks the transfer of vibrational energy out of the iodine stretch. Absorption recovery in  $I_2^-(Ar)_{20}$  (also a full solvent shell) occurs on a time scale of 130 ps.<sup>7</sup> Molecular dynamics simulations<sup>16</sup> and simulation of its FPE spectra<sup>11</sup> showed this time scale to be determined by the rate of vibrational relaxation on the ground state in conjunction with evaporation.

In all of these studies, the dynamics due to the upper-state processes of dissociation and recombination can be difficult to separate from those occurring on the ground state. In order to reduce the complexity of the system and examine only ground-state vibrational relaxation, we have paired FPES with femtosecond stimulated emission pumping (fs-SEP) and directly created vibrationally excited  $I_2^-$  in its ground electronic state embedded in a cluster of solvent molecules. In two recent papers,<sup>23,24</sup> we presented results for fs-SEP on the cluster  $I_2^-(CO_2)_4$ . Here, we continue this work by using fs-SEP to investigate vibrational relaxation in  $I_2^-(CO_2)_n$  ( $n=1,5$ ) and  $I_2^-(Ar)_n$  ( $n=1,2,6,9$ ).

The fs-SEP method is illustrated in Fig. 1. The potentials shown are those for bare  $I_2^-$ ; the addition of solvent molecules stabilizes the anion relative to the neutral by as much as 500 meV for 5  $CO_2$  molecules.<sup>25</sup> Ultrafast pump and dump laser pulses sequentially excite the  $I_2^-$  chromophore within the cluster to the  $\tilde{A}'^2\Pi_{g,1/2}$  electronic state, then stimulate a portion of the evolving wave packet back down

<sup>a)</sup>Current address: MPI für Kernphysik, Postfach 103980, 69029 Heidelberg, Germany.

<sup>b)</sup>Electronic mail: dan@radon.cchem.berkeley.edu

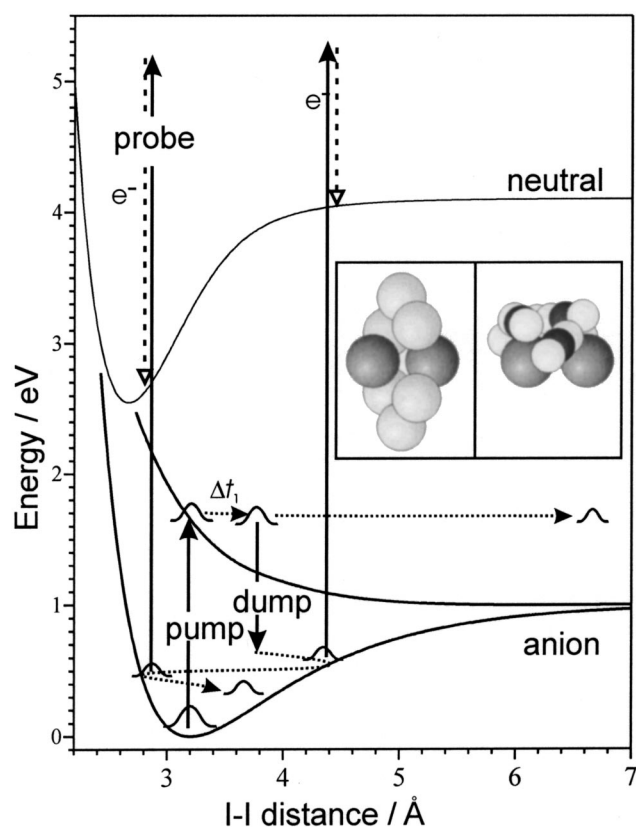


FIG. 1. Schematic of SEP-FPES experiment. Potential energy curves (bottom to top) are for the  $X\tilde{2}\Sigma_u^+$  and  $A'2\Pi_{g,1/2}$  states of  $I_2^-$  and  $X^1\Sigma_g^+$  state of  $I_2$ . The inset shows calculated structures for  $I_2^-(Ar)_6$  and  $I_2^-(CO_2)_5$  (Refs. 14, 17, 42).

to the ground  $X\tilde{2}\Sigma_u^+$  state. The resulting wave packet (the SEP wave packet) initially has vibrational excitation  $E_{exc} = h\nu_{pump} - h\nu_{dump}$ . The pump–dump delay  $\Delta t_1$  is chosen to optimize SEP efficiency and is generally around 100 fs.<sup>26</sup> As the wave packet evolves, energy transfer can occur between the vibrationally excited  $I_2^-$  and the surrounding solvent molecules. We probe the cluster at any time delay with a third ultrafast pulse, an UV probe pulse, which photodetaches the anion, promoting the cluster to the neutral state and producing a photoelectron whose energy depends on probe photon energy and the distance between the anion and neutral curves. The electrons are collected in a time-of-flight spectrometer, yielding PE spectra that depend on the dump–probe delay. Other groups using the fs-SEP method probe the vibrationally excited molecules with three-photon ionization<sup>27</sup> or time-resolved coherent anti-Stokes Raman spectroscopy.<sup>28,29</sup>

The PE spectra contain information about many attributes of the system: the SEP wave packet, the residual  $v = 0$  ground state wave packet, and the residual wave packet on the excited anion potential. However, when the SEP wave packet is at its inner turning point (ITP), photodetachment to the  $I_2$  ground state yields high kinetic energy electrons (see Fig. 1) that cannot be produced by any other photodetachment process, so that the highest energy region of the PE spectra enables one to track the dynamics at the ITP selectively. In previous work on  $I_2^-(CO_2)_4$ ,<sup>24</sup> we examined the

ITP region of the spectrum and found it indicative of energy loss to the solvent in two ways. Oscillations from recurrences of the SEP wave packet at the ITP were observed and exhibited a time-dependent increase in frequency as the  $I_2^-$  chromophore relaxed in the anharmonic well. In addition, relaxation caused the highest energy region of the PE spectrum to shift to lower energy as the anion wave packet moved further from the neutral surface.

Key results for  $I_2^-(CO_2)_4$  are as follows: Experiments were done at several excitation energies ( $E_{exc}$ ) up to 85% of the well depth (1.01 eV) for  $I_2^-$ , and the oscillations and spectral shifts were analyzed to determine the time-dependent vibrational energy  $E_{vib}(t)$ . We found that the chromophore loses  $\sim 0.2$  to  $0.4$  eV within the first 3 ps, and that the overall relaxation time scale was about 5 ps regardless of  $E_{exc}$ . This rate compares remarkably well with solution-phase experiments where the vibrational relaxation rate of ground state  $I_2^-$  in the lowest third of the potential well was found to occur with time constants of 3–6 ps.<sup>4,30–35</sup> We also found evidence for initial rapid energy loss during the first excursion of the wave packet across the potential, before its first arrival at the ITP 300–400 fs after the dump pulse. This observation is consistent with solution-phase results<sup>4,31,32</sup> and simulations of vibrational relaxation in clusters<sup>13</sup> and solution,<sup>36</sup> which indicate that energy loss at the top of the  $I_2^-$  potential well can be extremely efficient.

The  $I_2^-(CO_2)_4$  results form the basis for the current study of  $I_2^-(Ar)_n$  ( $n = 1, 2, 6, 9$ ) and  $I_2^-(CO_2)_n$  ( $n = 1, 5$ ). We are interested in how the vibrational relaxation dynamics change when the number and type of solvent molecules is varied. We also hope to gain more insight into two unresolved issues in the previous work: the apparent rapid energy loss during the first  $\sim 300$  fs, discussed earlier, and the time scale of solvent evaporation, a process strongly coupled to vibrational relaxation of the  $I_2^-$ . Product distributions<sup>37</sup> determined in our lab using a linear reflectron show that evaporation is largely complete in  $I_2^-(CO_2)_4$  and  $I_2^-(CO_2)_5$  several microseconds after excitation via fs-SEP, but the actual time scale for solvent evaporation from  $I_2^-(CO_2)_4$  could not be determined easily from the SEP-FPES spectra. Experiments and simulations of the photodissociation dynamics of  $I_2^-(CO_2)_n$  suggest that the  $CO_2$  solvent network has a relatively large capacity to absorb energy, whereas an argon solvent shell has a lower capacity due to much weaker intracuster bonding.<sup>7,11,12,16</sup> Both types of clusters are examined in the current study so that by comparing their dynamics we can determine the coupling of evaporation to vibrational relaxation with more certainty. The smallest clusters are of particular interest because complete evaporation is possible and no dynamics can occur once the solvent is gone; these clusters therefore provide definitive limits on the time scale for evaporation.

## II. EXPERIMENT

The apparatus has been described in detail previously.<sup>24</sup> An appropriate gas mixture (pure Ar at 30 psi or 2.5%  $CO_2$  in Ar at 20 psi) is passed over crystalline iodine, expanded into vacuum through a pulsed piezoelectric valve, and crossed by a 1.2 keV beam from an electron gun. Cluster

anions are pulse-extracted into a Wiley–McLaren mass spectrometer and travel to the laser interaction region. There, the cluster of interest is intersected by femtosecond pump, dump, and probe pulses generated from a Clark-MXR regeneratively amplified Ti:sapphire laser, which, like the pulsed valve, runs at a repetition rate of 500 Hz. The pump and probe pulse wavelengths are 790 nm (60  $\mu$ J, 90 fs), the fundamental of the Ti:sapphire laser, and 263 nm (20  $\mu$ J, 110 fs), produced by frequency-tripling some of the fundamental laser pulse. The tunable dump pulse (130 fs) is produced as the signal or idler beam from an optical parametric generator/amplifier (TOPAS; Light Conversion) pumped by a portion of the 790 nm pulse; the dump wavelength used in these studies is either 1250 nm (60  $\mu$ J), corresponding to  $E_{\text{exc}}=0.57$  eV, or 1520 nm (45  $\mu$ J), corresponding to  $E_{\text{exc}}=0.75$  eV. The pump–dump and dump–probe delays are independently set by propagating the pump and probe pulses through computer-controlled translation stages. Ejected electrons are collected with >50% efficiency in a magnetic bottle time-of-flight analyzer.

In experiments on  $\text{I}_2^-(\text{CO}_2)_n$  clusters, the dump pulse was chopped at half the laser repetition rate, with the two-color (pump+probe) spectra saved for normalization and simultaneously dynamically subtracted from the three-color spectra (pump+dump+probe) on a shot-to-shot basis. Typical collection times were 50 s per spectrum. The lower intensity of the  $\text{I}_2^-(\text{Ar})_n$  clusters made dynamical subtraction (and the corresponding loss of every other dump pulse) impractical. No subtraction or explicit normalization scheme was employed for these clusters; the spectra were normalized by scaling their total area. Average collection times for the  $\text{I}_2^-(\text{Ar})_n$  clusters were between 100 and 300 s per spectrum. The zeros-of-time inside the machine were determined by above-threshold-detachment of  $\text{I}^-$  by the dump and probe or pump and probe pulses.

### III. RESULTS

Representative PE spectra of  $\text{I}_2^-(\text{Ar})_2$ ,  $\text{I}_2^-(\text{Ar})_6$ , and  $\text{I}_2^-(\text{CO}_2)_5$  with  $E_{\text{exc}}=0.57$  eV are shown in Fig. 2. The x axis shows the electron kinetic energy (eKE). Spectra for the  $\text{I}_2^-(\text{Ar})_n$  clusters are taken with pump, dump, and probe pulses all present, and have been normalized to the total intensity. In the bottom panel, for  $\text{I}_2^-(\text{CO}_2)_5$ , dynamical subtraction, i.e., (pump+dump+probe)–(pump+probe) has been employed, and the three-color spectra were normalized to the two-color background spectra. Each panel shows spectra taken at three dump–probe delays. The results in Fig. 2 represent only a small sample of the overall data set; data for  $\text{I}_2^-(\text{Ar})$  were taken at  $E_{\text{exc}}=0.57$  eV, and data for  $\text{I}_2^-(\text{Ar})_{2,6,9}$  and  $\text{I}_2^-(\text{CO}_2)_{1,5}$  were taken 0.57 and 0.75 eV, with spectra obtained at hundreds of time delays for each cluster.

In the top panel of Fig. 2, spectra of  $\text{I}_2^-(\text{Ar})_2$  at short dump–probe delays are displayed. The pump–dump delay ( $\Delta t_1$  in Fig. 1) is 80 fs. The prominent peaks at eKE=1.6 and 0.7 eV are from detachment of the upper-state dissociation products,  $\text{I}^-$  and  $\text{I}^-(\text{Ar})$  in this case, and of a small amount of residual ground state  $\text{I}_2^-(\text{Ar})_2$ . Features induced by the dump pulse are of greatest interest for the current

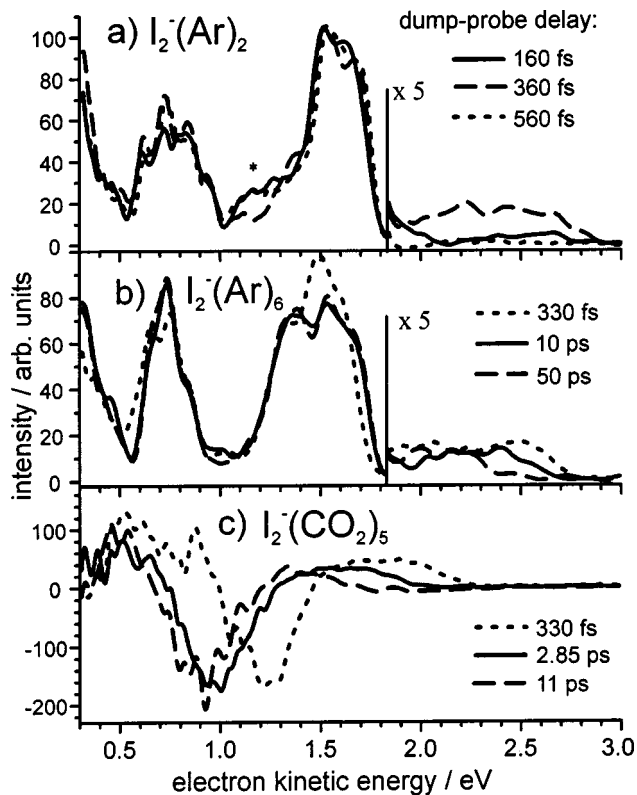


FIG. 2. Pump–dump–probe spectra for  $\text{I}_2^-(\text{S})_n$  with 0.57 eV initial excitation energy. (a)  $\text{I}_2^-(\text{Ar})_2$ , illustrating initial intensity oscillations. (b)  $\text{I}_2^-(\text{Ar})_6$ , demonstrating longer-time shifts of the high-eKE edge. (c)  $\text{I}_2^-(\text{CO}_2)_5$ , illustrating the results of dynamical subtraction and the more rapid edge shift.

study, most notably the signal at high electron kinetic energies (eKE). At 160 fs after the dump pulse, intensity at eKE >1.9 eV is relatively low, while at 360 fs a distinct feature is apparent in the region. The intensity at high eKE drops again in the 560 fs spectrum. The spectral region around 1.15 eV, marked with an asterisk, exhibits the opposite time-dependent behavior, i.e., has high intensity at 160 and 560 fs, but markedly lower intensity at 360 fs. These out-of-phase oscillations at high and lower eKE are from recurrences at the ITP and outer turning point of the SEP wave packet, respectively;<sup>24</sup> they are seen in bare  $\text{I}_2^-$  and for all the cluster sizes at both values of  $E_{\text{exc}}$ .

At dump–probe delays longer than a few picoseconds (3–9, depending on cluster size), oscillations are no longer evident, but in the larger clusters the high-eKE region of the spectrum continues to evolve, shifting to lower kinetic energies. This is illustrated in the middle and lower panels of Fig. 2, which show spectra of  $\text{I}_2^-(\text{Ar})_6$  and  $\text{I}_2^-(\text{CO}_2)_5$  at longer dump–probe delays. The pump–dump delays are 110 and 125 fs, respectively. The high-eKE feature shifts by about 0.4 eV in 50 ps for the argon cluster, and by 0.5 eV in 11 ps for the  $\text{CO}_2$  cluster. The  $\text{I}_2^-(\text{Ar})_6$  spectra are qualitatively similar to the  $\text{I}_2^-(\text{Ar})_2$  spectra in the top panel, with the most prominent peaks being dissociation products induced by the pump pulse. The  $\text{I}_2^-(\text{CO}_2)_5$  spectra, as mentioned previously, are dynamically subtracted, so regions of positive intensity correspond to features induced by the dump pulse, while the

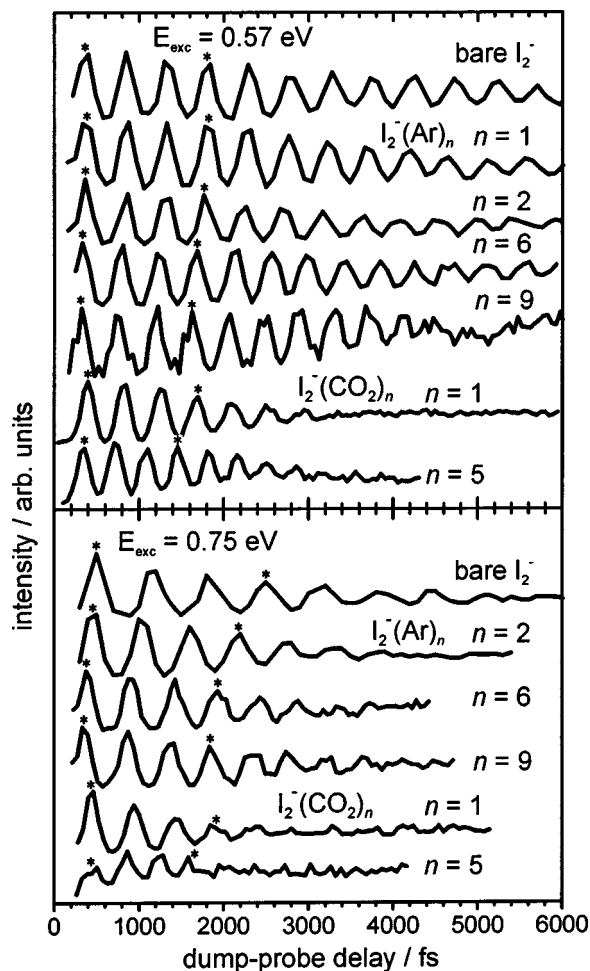


FIG. 3. Integrated high-eKE signal for bare and clustered  $I_2^-$  as a function of time. Top panel:  $E_{exc}=0.57$  eV; bottom panel:  $E_{exc}=0.75$  eV.

negative-going regions are due to depletion of the upper-state wave packet (i.e., dissociation products) by the dump pulse. In both cases the high-eKE portion of the spectrum is induced by the dump pulse.

The oscillations at high eKE can be followed by plotting the integrated intensity of the high-eKE signal as a function of time. Results for bare  $I_2^-$ ,  $I_2^-(Ar)_{2,6,9}$  and  $I_2^-(CO_2)_{1,5}$  at  $E_{exc}=0.57$  and  $0.75$  eV are shown in Fig. 3; similar plots for  $I_2^-(CO_2)_4$  appear in our previous paper.<sup>24</sup> The top panel of Fig. 3 also shows high eKE oscillations from  $I_2^-(Ar)$ , which was studied only at  $E_{exc}=0.57$  eV. The frequency and dephasing time of  $I_2^-(Ar)$  are essentially identical to those of bare  $I_2^-$ . However, in  $I_2^-$ , the oscillations rephase around 45 ps<sup>38</sup> with intensity comparable to the initial magnitude, while no rephasing is seen in  $I_2^-(Ar)$ .

The oscillations for the other clusters show significant differences from bare  $I_2^-$ . The trends are most easily discerned by examining them in groups by solvent type and by  $E_{exc}$ , and are highlighted in Fig. 3 by asterisk symbols placed over the first and fourth maximum for each oscillation. For both  $I_2^-(Ar)_{n \geq 2}$  and  $I_2^-(CO_2)_{n \geq 1}$  clusters at a given value of  $E_{exc}$ , the spacing between the intensity maxima decreases with increasing  $n$ ; in other words, the oscillation frequency increases with the addition of solvent atoms or

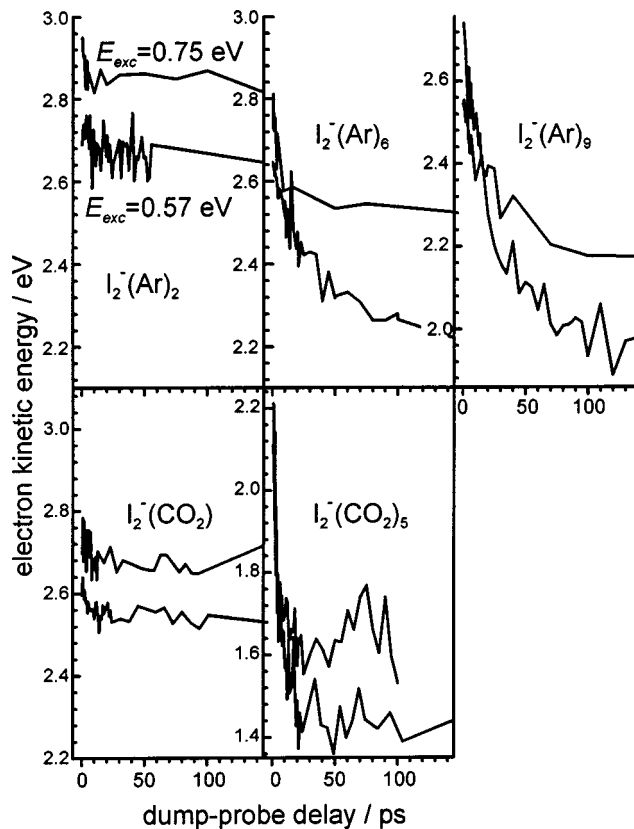


FIG. 4. Position of the high-eKE edge of the spectrum as function of dump-probe delay time. Each panel shows a different cluster, with the upper trace at  $E_{exc}=0.75$  eV and the lower trace at  $E_{exc}=0.57$  eV.

molecules. Comparison of the same cluster size (including  $n=0$ ) at different values of  $E_{exc}$  shows that a cluster excited with  $0.75$  eV has a lower oscillation frequency than at  $E_{exc}=0.57$  eV. Different clusters lose coherence over different time scales: the  $I_2^-(Ar)_n$  oscillations dephase more quickly for  $E_{exc}=0.75$  eV than for  $E_{exc}=0.57$  eV (4 ps versus at least 6 ps); this trend does not exist to the same degree in the  $CO_2$  cluster oscillations, which generally dephase around 3 ps for both values of  $E_{exc}$ . A single  $CO_2$  molecule reduces the dephasing time more than nine argon atoms, but for both solvent types the dephasing time at the two excitation energies is shorter than for that of  $I_2^-$ , about 7–9 ps, which results from anharmonic dephasing of the SEP wave packet.<sup>38</sup> Finally, the most important but least obvious characteristic of all the cluster oscillations in Fig. 3 [with the exception of  $I_2^-(Ar)$ ] is that their frequency increases with time, as seen previously<sup>24</sup> for  $I_2^-(CO_2)_4$  and discussed in the following.

The other dump-induced effect is the shift of the high-eKE edge of the spectrum toward lower eKE with increasing dump-probe delay. In Fig. 4, the position of this edge (where “edge” is the energy at the half-height of the high-eKE intensity) is graphed as a function of dump-probe delay out to 150 ps for each cluster and value of  $E_{exc}$ . Each panel displays the shift for one cluster, with the upper trace corresponding to  $E_{exc}=0.75$  eV, and the lower curve to  $E_{exc}=0.57$  eV. For  $I_2^-(Ar)_2$  at both values of  $E_{exc}$  and  $I_2^-(Ar)_{6,9}$  and  $I_2^-(CO_2)$  at  $E_{exc}=0.57$  eV, very noisy data at early times

(<7 ps) have been smoothed with a period of about 500 fs. Similar plots for bare  $I_2^-$  and  $I_2^-(CO_2)_4$  can be found in our previous publication.<sup>24</sup>  $I_2^-(Ar)$  with  $E_{exc}=0.57$  eV does not undergo a measurable spectral shift and is not shown.  $I_2^-(Ar)_2$  at  $E_{exc}=0.57$  eV undergoes a very small shift of around 50 meV within the first 15 ps.  $I_2^-(CO_2)$  at both values of  $E_{exc}$  and  $I_2^-(Ar)_2$  at the higher excitation energy undergo small but distinct shifts of about 0.1 eV within the first 15 ps. In contrast, the shift of the high-eKE edge of the spectrum in larger clusters is quite substantial, ranging from about 0.25 eV for  $I_2^-(Ar)_6$  with  $E_{exc}=0.57$  eV to about 0.6 eV for  $I_2^-(Ar)_9$  and  $I_2^-(CO_2)_5$  with  $E_{exc}=0.75$  eV. The shifts for  $I_2^-(CO_2)_5$  happen much more quickly than for the larger argon cluster spectra; for  $I_2^-(CO_2)_5$  at both excitation energies, the spectra no longer shift by about 30 ps, while for  $I_2^-(Ar)_9$  at both energies and  $I_2^-(Ar)_6$  at  $E_{exc}=0.57$  eV, shifting does not appear to be over even by 100 ps.

#### IV. ANALYSIS

Procedures for analysis of the time-dependent oscillations and shifts that were employed for  $I_2^-(CO_2)_4$  are also utilized here.<sup>24</sup> The high-eKE signal, which is the focus of our analysis, is from detachment of the SEP wave packet near the ITP of the ground state anion potential, as illustrated in Fig. 1; any electrons with eKE above about 2 eV [lower for  $I_2^-(CO_2)_5$ , since the anion is shifted so much relative to the neutral] must come from vibrationally excited  $I_2^-$ . Elsewhere on the anion ground state, detachment of the SEP wave packet results in slower electrons which are generally in the same eKE range as electrons detached from the upper state or residual  $v=0$  wave packets. Only at high eKE do the spectra exhibit “clean” SEP dynamics that can be readily analyzed. We fit the intensity oscillations and spectrum edge shifts in this region to determine the time-dependent  $I_2^-$  vibrational energy,  $E_{vib}(t)$ , and compare the rates and amounts of energy loss in the various clusters. For each cluster, we can also use the values of  $E_{vib}$  derived in both ways to come up with quantitative measures for the amount of energy lost before the first occurrence of the wave packet at the ITP, and, in some cases, for the total amount of energy lost in the system.

##### A. Oscillations at the inner turning point

The oscillations shown in Fig. 3 occur as the SEP wave packet moves into and out of the ITP region. In bare  $I_2^-$ , the oscillation frequency at a given  $E_{exc}$  is constant, decreasing with increasing  $E_{exc}$  owing to the anharmonicity of the potential.<sup>38</sup> In contrast, we found that in  $I_2^-(CO_2)_4$ , the oscillation frequency increases with time,<sup>23,24</sup> since in losing energy to the solvent modes the  $I_2^-$  wave packet drops down in the anharmonic potential well, where the spacing between adjacent vibrational levels is larger. The oscillation frequency also increases with time for all clusters discussed here, except for  $I_2^-(Ar)$  at  $E_{exc}=0.57$  eV. In order to quantify the changing frequency, each oscillation in Fig. 3 was fit to a modified sinusoidal function with a frequency that increases either linearly or quadratically with time. Before fitting, the oscillations were shifted to be centered about zero

TABLE I. Selected parameters from fits to oscillations in Fig. 3, after smoothing. See Eq. (1) in text and Fig. 5.

$E_{exc}$ (eV)	Cluster	$f_0$ (cm <sup>-1</sup> )	$a$ (cm <sup>-1</sup> /ps)	$b$ ((cm <sup>-1</sup> ) <sup>2</sup> /ps)
0.57	Bare $I_2^-$ <sup>a</sup>	69	...	...
	$I_2^-(Ar)$	69.7±0.2	0.13±0.05	...
	$I_2^-(Ar)_2$	70.2±0.2	0.74±0.09	...
	$I_2^-(Ar)_6$	73.0±0.3	1.4±0.1	...
	$I_2^-(Ar)_9$	74.5±0.3	2.25±0.13	...
	$I_2^-(CO_2)$	74.7±0.4	2.3±0.4	...
		72.8±1.3	5.6±2	$-1.1 \times 10^{-3} \pm 7 \times 10^{-4}$
	$I_2^-(CO_2)_4$ <sup>b</sup>	78.6±0.3	6.7±0.3	...
	$I_2^-(CO_2)_5$	84.0±0.3	5.6±0.2	...
0.75	Bare $I_2^-$ <sup>a</sup>	52	...	...
	$I_2^-(Ar)_2$	56.8±0.5	0.85±0.31	...
	$I_2^-(Ar)_6$	59.7±0.4	4.2±0.3	...
		62.8±0.9	-0.34±0.13	$1.3 \times 10^{-3} \pm 3.7 \times 10^{-4}$
	$I_2^-(Ar)_9$	60.8±0.4	4.9±0.2	...
	$I_2^-(CO_2)$	63.7±0.5	3.7±0.3	...
		61.9±1.2	6.5±1.8	$-8.4 \times 10^{-4} \pm 5.4 \times 10^{-4}$
	$I_2^-(CO_2)_4$ <sup>b</sup>	79.4±1.0	1.4±0.7	...
	$I_2^-(CO_2)_5$	80.5±1.5	5.0±1.1	...

<sup>a</sup>Reference 38.

<sup>b</sup>Reference 24.

intensity, and a FFT filter was applied that passed bandwidth between 0.5 and 1.5 times the peak in the overall FT. After smoothing, each oscillation was fit by a nonlinear least-squares method with a function proportional to

$$\left[ \exp\left(\frac{-(t-t_0)^2}{2w^2}\right) + y_0 \right] \sin\left(2\pi t \left(f_0 + \frac{a}{2}t + \frac{b}{3}t^2\right) + \phi\right). \quad (1)$$

The instantaneous, time-dependent frequency is determined by the derivative of the argument,  $f_0 + at + bt^2$ . The envelope is an offset Gaussian function, needed because the intensity does not decay to zero and, for several data sets, peaks at the second oscillatory maximum. Selected parameters resulting from the fits are shown in Table I, and the time-dependent frequencies are plotted in Fig. 5. Also included are the constant frequencies for bare  $I_2^-$  and the linearly increasing frequencies for  $I_2^-(CO_2)_4$  determined previously.<sup>24</sup> Each oscillation was fit first with  $b=0$  (linearly changing frequency), and then a fit with  $b \neq 0$  (quadratically changing frequency) was attempted. In most cases, the quadratically changing frequency did not result in a better fit. However for  $I_2^-(CO_2)$  at both values of  $E_{exc}$  and for  $I_2^-(Ar)_6$  at  $E_{exc}=0.75$  eV, the quadratically changing frequency produced a fit that was both better than and different from the fit with the linearly changing frequency. In these cases, parameters for both fits are listed in Table I, but for simplicity the quadratic fits are not displayed in Fig. 5. Generally, the oscillations in the clusters with  $E_{exc}=0.75$  eV increase in frequency more quickly than those at the lower excitation energy, except for  $I_2^-(CO_2)_4$ , where the slope at  $E_{exc}=0.75$  eV (from the previous paper<sup>24</sup>) now looks anomalously low in light of the additional data for  $I_2^-(CO_2)_5$ . A common characteristic of the fits to all of the clusters is that

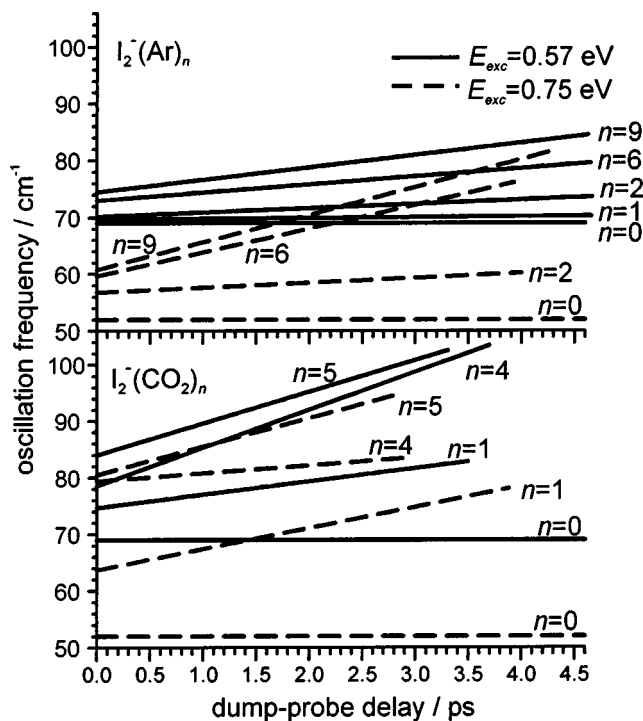


FIG. 5. Time dependent oscillation frequencies  $f_0 + at$  [see Eq. (1) and Table I] for  $I_2^-(Ar)_n$  (top panel) and  $I_2^-(CO_2)_n$  (bottom panel) at  $E_{exc} = 0.57$  eV (solid lines) and 0.75 eV (dashed lines).

extrapolation to  $t=0$  yields a higher frequency than bare  $I_2^-$  at the same value of  $E_{exc}$ ; this is particularly pronounced for the  $I_2^-(CO_2)_{4,5}$  clusters.

The instantaneous frequency of the oscillations depends on the spacing between adjacent vibrational energy levels in the  $I_2^-$  moiety. Thus, using the known potential for bare  $I_2^-$ ,<sup>38</sup> the time-dependent frequencies can be converted to time-dependent vibrational energies [ $E_{vib}(t)$ ]. Values of  $E_{vib}(t)$  determined from the linearly increasing frequency fits for  $I_2^-(Ar)_n$  and  $I_2^-(CO_2)_n$  clusters are shown in Fig. 6 as heavy straight lines. When the oscillation frequency increases with time,  $E_{vib}(t)$  decreases.  $E_{vib}$  can be determined in this manner only while the oscillations have measurable amplitude, and so is shown up to 3–4 ps for the  $CO_2$  clusters and 4–7 ps for the Ar clusters. The decrease in  $E_{vib}$  is somewhat more pronounced for  $E_{exc} = 0.75$  eV than 0.57 eV, and generally faster for larger clusters. For the argon clusters, the losses range from 34 meV over 4 ps (for  $n=2$  at  $E_{exc} = 0.75$  eV) to 240 meV over 4.3 ps (for  $n=9$  at  $E_{exc} = 0.75$  eV). The loss for  $I_2^-(Ar)$ , for which the oscillation frequency shows no significant change with time, would be negligible. For the  $CO_2$  clusters,  $E_{vib}$  derived from the oscillations shows losses that range from 70 meV over 3.5 ps ( $n=1$ ,  $E_{exc} = 0.57$  eV, quadratic fit) to 290 meV over 4.2 ps ( $n=5$ ,  $E_{exc} = 0.75$  eV). Note that these losses are all measured from the extrapolated values to  $t=0$  of the linear fits, all of which are lower than the known initial  $E_{exc}$ . We have attributed this discrepancy to initial fast energy loss before the first arrival of the wave packet at the inner turning point, unseen in our analysis because we only detect at the ITP.<sup>24</sup> This point is discussed further in Sec. IV C.

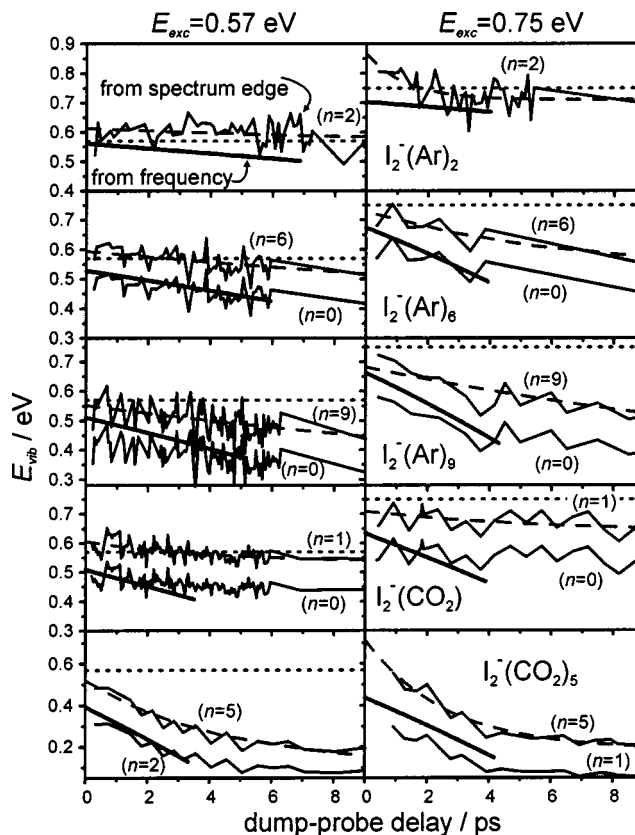


FIG. 6. Vibrational energy ( $E_{vib}$ ) remaining for the cluster at early dump-probe delay times. Each cluster size is on a separate row. Jagged lines are derived from the shift of the spectrum edge in Fig. 4, the uppermost assuming no evaporation ( $n=n_i$ ), and the lower either assuming total evaporation [ $I_2^-(Ar)_n$  and  $I_2^-(CO_2)$ ] or the smallest product found in the microsecond product distributions—Ref. 34 [ $I_2^-(CO_2)_5$ ]. The smooth dashed curve through the  $n_i$  curves in each panel represents an exponential fit using Eq. (2); parameters are given in Table II. The straight solid lines are derived from the time-dependent frequency of the oscillations using the potential for bare  $I_2^-$ .  $E_{exc} = h\nu_{pump} - h\nu_{dump}$  is shown as a horizontal dotted line.

## B. Shift of the spectrum

The amount of vibrational energy in the  $I_2^-$  moiety can also be determined by the position of the high-eKE edge of the spectrum, because greater vibrational excitation yields more energetic photoelectrons at the inner turning point. Thus the shift of the spectrum edge to lower energies, as seen in Fig. 4, signifies vibrational relaxation in the  $I_2^-$  well, and we can use the known potentials for bare  $I_2^-$  and neutral  $I_2$ ,<sup>38–41</sup> coupled with the known “solvent shifts” in the PE spectrum induced by clustering,<sup>25,42</sup> to extract time-dependent values of  $E_{vib}$  for each cluster.

The edge position is given by  $h\nu_{probe} - VDE_{ITP}$ , where  $h\nu_{probe}$  is the energy of the probe photon and  $VDE_{ITP}$  is the vertical detachment energy at the inner turning point.  $VDE_{ITP}$  is determined both by  $E_{vib}$  and by the solvent shift for the cluster of interest; the larger the cluster, the more the anion is stabilized relative to the neutral surface. Addition of 2, 6, and 9 argon atoms shifts the anion potential lower with respect to the ground neutral state by 50, 130, and 160 meV, respectively,<sup>42</sup> while the addition of 1 and 5  $CO_2$  molecules shifts the anion by 140 and 500 meV.<sup>25</sup> Since evaporation, which would change the solvent shift, is a possibility,  $E_{vib}$

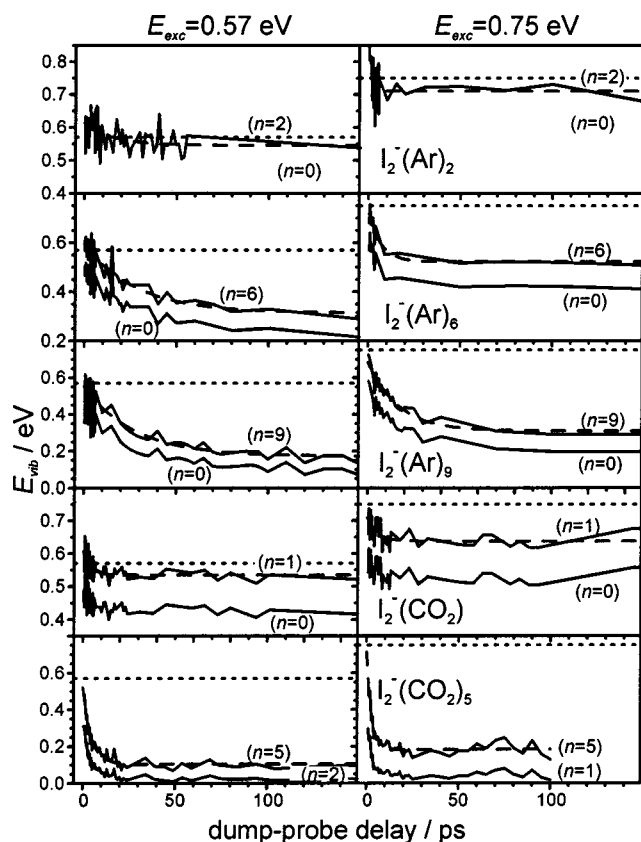


FIG. 7.  $E_{\text{vib}}(t)$  over long times for clustered  $\text{I}_2^-$ , determined from the shift of the spectrum edge. Lines are as described in the caption for Fig. 6.

must be calculated assuming all possible values for the number of solvent atoms/molecules.

The resulting values of  $E_{\text{vib}}(t)$  are shown as the jagged lines in Fig. 6, for short dump-probe delay times, and in Fig. 7, for times out to 150 ps. Note that different vertical scales are used in these figures, depending on the cluster identity. For the  $\text{I}_2^-(\text{Ar})_n$  clusters,  $E_{\text{vib}}$  was calculated for each value of  $n \geq 0$  up to the initial cluster size,  $n_i$ , since based on the binding energy of Ar to  $\text{I}_2^-$ , even the lower  $E_{\text{exc}}$  of 0.57 eV is theoretically enough to evaporate all of the solvent atoms from the largest cluster,  $n=9$ . However, for clarity only the curves for  $E_{\text{vib}}$  assuming  $n=0$  and  $n=n_i$  are displayed; the curves for the intermediate cluster sizes are more-or-less evenly spaced between the two shown. For the  $\text{I}_2^-(\text{CO}_2)_5$  clusters, the minimum size cluster shown in Figs. 6 and 7 is determined by the smallest significant product found in the daughter ion distribution at the excitation energy in question.<sup>37</sup> For  $\text{I}_2^-(\text{CO}_2)$ , curves are shown for the binary complex and the bare ion.

For each cluster and value of  $E_{\text{exc}}$ ,  $E_{\text{vib}}$  for  $n_i$  was fit to a single exponential decay curve of the form

$$E_{\text{vib}}(t) = E_0 + A e^{-t/\tau}. \quad (2)$$

The best fit is shown as a dashed line through the corresponding  $n_i$  curve. The fit parameters, including those determined previously for  $\text{I}_2^-(\text{CO}_2)_4$ ,<sup>24</sup> can be found in Table II. For each  $\text{I}_2^-(\text{CO}_2)_n$  cluster except  $n=5$  at  $E_{\text{exc}}=0.75$  eV, the time constant for vibrational relaxation,  $\tau$ , is between 4 and 6 ps, relatively independent of  $E_{\text{exc}}$  or  $n$ . In contrast,  $\tau$  for

TABLE II. Parameters for exponential fit of the form  $E_{\text{vib}} = E_0 + A e^{-t/\tau}$  to uppermost  $E_{\text{vib}}$  curves in Figs. 6 and 7.

$E_{\text{exc}}$ (eV)	Cluster	$E_0$ (eV)	$A$ (eV)	$\tau$ (ps)
0.57	$\text{I}_2^-(\text{Ar})_2$	$0.545 \pm 0.012$	$0.068 \pm 0.013$	$15 \pm 9$
	$\text{I}_2^-(\text{Ar})_6$	$0.314 \pm 0.015$	$0.280 \pm 0.014$	$28.2 \pm 3.8$
	$\text{I}_2^-(\text{Ar})_9$	$0.171 \pm 0.015$	$0.381 \pm 0.014$	$27.6 \pm 4.0$
	$\text{I}_2^-(\text{CO}_2)$	$0.535 \pm 0.004$	$0.072 \pm 0.007$	$3.9 \pm 0.8$
	$\text{I}_2^-(\text{CO}_2)_4^a$	$0.147 \pm 0.005$	$0.422 \pm 0.007$	$5.0 \pm 0.2$
0.75	$\text{I}_2^-(\text{Ar})_2$	$0.710 \pm 0.011$	$0.157 \pm 0.050$	$1.3 \pm 0.6$
	$\text{I}_2^-(\text{Ar})_6$	$0.523 \pm 0.013$	$0.207 \pm 0.024$	$6.4 \pm 2.1$
	$\text{I}_2^-(\text{Ar})_9$	$0.309 \pm 0.017$	$0.373 \pm 0.019$	$16.4 \pm 2.1$
	$\text{I}_2^-(\text{CO}_2)$	$0.637 \pm 0.006$	$0.072 \pm 0.017$	$5.6 \pm 2.4$
	$\text{I}_2^-(\text{CO}_2)_4^a$	$0.193 \pm 0.006$	$0.47 \pm 0.02$	$5.16 \pm 0.39$
	$\text{I}_2^-(\text{CO}_2)_5$	$0.183 \pm 0.005$	$0.530 \pm 0.039$	$2.62 \pm 0.25$

<sup>a</sup>Reference 24.

$\text{I}_2^-(\text{Ar})_n$  appears to depend strongly on both  $n$  and  $E_{\text{exc}}$ ; for any size  $n$ , increasing  $E_{\text{exc}}$  decreases  $\tau$  (i.e., the dynamics speed up at higher excitation energy). Alternatively, at a given value of  $E_{\text{exc}}$ , increasing the cluster size tends to increase  $\tau$ , except for  $n=6$  and  $9$  at  $E_{\text{exc}}=0.57$  eV, which have approximately the same value of  $\tau$ . For either solvent type, as the number of solvent molecules increases, the residual energy  $E_0$  decreases. The constant  $A$  represents a lower bound for the total amount of energy loss from the iodine vibration, regardless of whether evaporation has occurred. It increases with cluster size except for  $\text{I}_2^-(\text{CO}_2)_4$  and  $\text{I}_2^-(\text{CO}_2)_5$ , for which it is approximately the same.

### C. Upper and lower bounds of $E_{\text{vib}}(t)$

As discussed previously,<sup>24</sup> values of  $E_{\text{vib}}$  derived from the oscillations and edge-shifts are lower and upper bounds, respectively, to the “true” amount of energy remaining in the  $\text{I}_2^-$  vibration. Previous resonance impulsive stimulated Raman scattering (RISRS) experiments<sup>43</sup> showed that the fundamental oscillation frequencies of  $\text{I}_2^-(\text{CO}_2)_{n \geq 4}$  and  $\text{I}_2^-(\text{Ar})_{n \geq 12}$  are slightly blueshifted [ $1.7 \text{ cm}^{-1}$  for  $\text{I}_2^-(\text{CO}_2)_4$ ,  $1 \text{ cm}^{-1}$  for  $\text{I}_2^-(\text{Ar})_{12}$ ] compared to bare  $\text{I}_2^-$ , while no blueshift was seen for  $\text{I}_2^-(\text{Ar})_6$ . Since we use the bare  $\text{I}_2^-$  potential to determine  $E_{\text{vib}}$  from the oscillations, the vibrational energy remaining is underestimated in those clusters that show a blueshift. However,  $\text{I}_2^-(\text{CO}_2)_{4,5}$  are the only clusters considered here which we know are blueshifted; RISRS spectra were not measured for  $\text{I}_2^-(\text{CO}_2)$  or  $\text{I}_2^-(\text{Ar})_9$ , but the blueshifts for these clusters are certainly less than those of  $\text{I}_2^-(\text{CO}_2)_4$  and  $\text{I}_2^-(\text{Ar})_{12}$ , respectively. Thus, for analysis purposes, we will neglect this effect for clusters other than  $\text{I}_2^-(\text{CO}_2)_{4,5}$ , keeping in mind that our experiments probe high vibrational levels where solvent effects on the  $\text{I}_2^-$  vibrational frequency may be amplified. On the other hand, our extraction of  $E_{\text{vib}}$  from the maximum eKE in the FPE spectra overestimates it for all clusters reported here; the spectra are Doppler-broadened because of the speed of the ion beam,<sup>44</sup> and the edge of the spectrum that we measure is actually higher in energy than the true energy from detachment at the ITP.

Values of  $E_{\text{vib}}$  from the edge shifts are also upper limits for reasons that were not considered previously. In constructing Figs. 6 and 7, we assume that the edge position is a function only of the vibrational energy of the  $I_2^-$  and the number of solvent species present at time  $t$ ; the only effect of the solvent is to shift the anion potential lower in energy relative to the neutral, using energetics derived from the PE spectra of relatively cold cluster anions. However, in our experiment, the cluster heats up as the  $I_2^-$  loses energy (but before evaporation occurs), so the observed spectra reflect vibrational excitation not only of the  $I_2^-$  but of the low-frequency anion-solvent and solvent-solvent vibrational modes. Since the frequency of anion-solvent modes will be higher, in general, than the frequencies of the analogous modes in the neutral, vibrational excitation of these modes will shift the maximum eKE out to higher values, even if  $\Delta v = 0$  transitions in these modes dominate. Thus, the value of  $E_{\text{vib}}$  derived assuming only  $I_2^-$  vibrational excitation will be too high. As the clusters lose energy by evaporative cooling, this effect becomes less important. As a consequence, the distinction is blurred between a hot cluster with  $n$  solvent species and a cluster with  $n-1$  solvents resulting from evaporative cooling, so that abrupt edge shifts associated with solvent evaporation should not be (and indeed never are) observed.

Figure 5 shows that by the time the wave packet first arrives at the inner turning point of the iodine potential ( $\sim 300$ – $400$  fs as seen in Fig. 3), its oscillation frequency is already significantly higher than that of bare  $I_2^-$  at the same  $E_{\text{exc}}$ . If the frequency corresponds directly to  $E_{\text{vib}}$ , this means that the  $I_2^-$  has rapidly lost energy during the first half-oscillation across the potential, which we do not probe in our analysis of the high-eKE region of the spectrum. For  $I_2^-(Ar)_{2,6,9}$  and  $I_2^-(CO_2)$ , converting the frequency at this first ITP occurrence directly into  $E_{\text{vib}}$  and subtracting the result from the known value of  $E_{\text{exc}}$  (0.57 or 0.75 eV) gives the apparent energy loss during the first partial oscillation. These values are given in Table III. They range from only 10 meV for  $I_2^-(Ar)_2$  to 135 meV for  $I_2^-(CO_2)$ . Also given in Table III are values for  $I_2^-(CO_2)_{4,5}$ , where we provide a range for the initial energy loss, bracketing it with the values of  $E_{\text{vib}}(t=0)$  derived from the oscillations (the higher values) and edge shifts.

At longer times, once the oscillations have dephased, we can only use the edge shifts to determine  $E_{\text{vib}}(t)$ , the values of which represent upper bounds for the reasons discussed earlier. However, for clusters where the frequency blueshifting is minimal, we can use the oscillation-derived values of  $E_{\text{vib}}$  to estimate a correction to the edge-based values of  $E_{\text{vib}}(t)$  at short times (while the oscillations are still occurring), and extend the correction to longer times, after the oscillations have dephased. The most appropriate way to correct the edge-derived values is to shift the raw electron kinetic energy values of the edge position (Fig. 4) lower in energy to compensate for the broadening of the spectra; the necessary shift can be determined by the frequency-derived  $E_{\text{vib}}$ . Then the shifted eKE values can be reconverted to  $E_{\text{vib}}$ . We have done this for  $I_2^-(CO_2)$  and the  $I_2^-(Ar)_n$  clusters, for which the blueshift of the oscillation frequency

TABLE III. Short- and long-time values for energy losses from the iodine stretch.

$E_{\text{exc}}$ (eV)	Cluster	First ITP occurrence (fs)	Initial energy loss <sup>a</sup> (meV)	Long-time energy loss <sup>b</sup> (meV) (zero, max evaporation)
0.57	$I_2^-(Ar)_2$	360	10	75, 110
	$I_2^-(Ar)_6$	330	50	310, 380
	$I_2^-(Ar)_9$	320	70	425, 490
	$I_2^-(CO_2)$	400	70	130, 230
	$I_2^-(CO_2)_{4,5}^c$	350	30–140	>420, >530
	$I_2^-(CO_2)_5$	330	80–200	>470, >540
0.75	$I_2^-(Ar)_2$	450	50	155, 190
	$I_2^-(Ar)_6$	380	100	280, 370
	$I_2^-(Ar)_9$	330	100	460, 550
	$I_2^-(CO_2)$	460	135	200, 305
	$I_2^-(CO_2)_{4,5}^c$	420	120–300	>560, >720
	$I_2^-(CO_2)_5$	440	120–340	>570, >700

<sup>a</sup>Initial energy loss at first ITP occurrence determined using equality of oscillation-derived  $E_{\text{vib}}$  (normal type), or through bracketing the true  $E_{\text{vib}}$  between oscillation-derived and edge-derived  $E_{\text{vib}}$  (*italics*).

<sup>b</sup>Long-time energy loss. Assumed to be exact for  $I_2^-(CO_2)$  and  $I_2^-(Ar)_n$  based on the corrected edge-derived  $E_{\text{vib}}$  values. For  $I_2^-(CO_2)_{4,5}$ , the values are minimum energy loss based only on raw edge-derived  $E_{\text{vib}}$ . In both cases, the first number presumes no evaporation, and the second presumes complete evaporation to the smallest- $n$  curve in Fig. 7.

<sup>c</sup>Reference 24.

should be unimportant. For example, we find for  $I_2^-(CO_2)$  with  $E_{\text{exc}} = 0.57$  eV that the edge position must be shifted lower in eKE by 0.136 eV to make the edge-derived value of  $E_{\text{vib}}$  at 400 fs (the first occurrence at the ITP) match the frequency-derived value at this time. The appropriately shifted values of eKE yield for each cluster and excitation energy new values of  $E_{\text{vib}}$ , which can be fit by an exponential decay function [Eq. (2)]. For all clusters, the time constant  $\tau$  was not significantly changed from the values in Table II; the asymptotic energy  $E_0$  is moderately reduced (by 6%–18%), and the amount of energy lost,  $A$ , is slightly reduced (by 2%–8%).

These corrections improve the accuracy of values for the amount of energy loss at long times, or at least times long compared to  $\tau$ . Such values can be obtained from the asymptotic  $E_0$  values of exponential fits to the corrected  $E_{\text{vib}}(t)$  curves, assuming either no evaporation or complete evaporation. For example, the corrected values for  $I_2^-(CO_2)$  with  $E_{\text{exc}} = 0.57$  eV indicate that, assuming no evaporation, 130 meV is transferred out of the iodine stretch, or 230 meV if evaporation is assumed. At 0.75 eV initial excitation, the energy loss is 200 or 305 meV without or with evaporation of the single solvent molecule. Values of this long-time energy loss in  $I_2^-(CO_2)$  and  $I_2^-(Ar)_n$  are presented in Table III. This procedure cannot be applied to  $I_2^-(CO_2)_{4,5}$  because of the solvent-induced blueshift. The values for long-time energy loss for these species in Table III are taken solely from the (uncorrected) edge-derived  $E_{\text{vib}}$ , which overestimates the amount of energy remaining in the  $I_2^-$  vibration, and thus represent lower bounds.

## V. DISCUSSION

In many ways, our results conform to expectations for energy relaxation dynamics in clusters. Vibrational energy loss is significantly faster in  $I_2^-(CO_2)_n$  clusters than in  $I_2^-(Ar)_n$  clusters, a result that can be understood in terms of stronger chromophore–solvent coupling and higher densities of solvent intermolecular vibrational states in  $I_2^-(CO_2)_n$  clusters. As the number of a particular type of solvent species is increased, the density of solvent vibrational states goes up, as does the rate of vibrational energy transfer. These trends are covered in more detail in the discussion that follows.

One important aspect of the overall dynamics not probed directly in our experiments is the ultimate disposal of solvent vibrational energy via evaporative cooling. In contrast to the vibrational energy loss, the stronger solvent binding and larger density of vibrational states in  $I_2^-(CO_2)_n$  clusters should lead to slower evaporation than from  $I_2^-(Ar)_n$  clusters. As a consequence, in large  $I_2^-(CO_2)_n$  clusters, one expects a significant separation of time scales between rapid vibrational energy relaxation of the  $I_2^-$  and much slower solvent evaporation, in which case a statistical treatment would suffice to yield approximate solvent evaporation rates. Such a treatment was applied in our recent study of  $I_2^-(CO_2)_{4,5}$  to model the extent (but not the rate) of solvent evaporation as a function of initial  $I_2^-$  excitation energy.<sup>37</sup> On the other hand,  $I_2^-(CO_2)$  is too small to warrant a statistical treatment, as are the two smallest Ar clusters,  $I_2^-(Ar)_{1,2}$ . Analysis of the FPE spectra of larger  $I_2^-(Ar)_n$  clusters<sup>11</sup> showed that vibrational energy relaxation and solvent evaporation occurred on similar time scales, complicating a statistical treatment of the solvent evaporation.

We are therefore particularly interested in determining as much as possible from our experimental data concerning the time scale of evaporation. As long as the spectra continue to evolve, either by showing an increasing oscillation frequency or a shifting of the spectrum edge, there must be at least one solvent species left to be driving the energy loss, so our results provide a lower bound for the time required for complete evaporation. We first consider the smallest clusters,  $I_2^-(Ar)_{1,2}$  and  $I_2^-(CO_2)$ , which have little or no solvent network in which energy can be stored. We next discuss  $I_2^-(CO_2)_5$  in the context of the previous work on  $I_2^-(CO_2)_4$ , which showed evidence for a large role of the solvent network in energy absorption. Finally, we consider  $I_2^-(Ar)_6$  and  $I_2^-(Ar)_9$ , whose dynamics indicate intermediate solvent network effects.

### A. $I_2^-(Ar)$ and $I_2^-(Ar)_2$

A single argon atom seems to have very little effect on vibrationally excited  $I_2^-$  during the initial oscillation: the oscillation frequency only increases by about  $1\text{ cm}^{-1}$  during the 9 ps over which oscillations can be seen, the dephasing time is the same as for bare  $I_2^-$ , and the edge of the spectrum undergoes no observable shift to lower energy. At longer times, the cluster oscillations do not rephase, though in the bare ion they rephase by 45 ps.<sup>38</sup> The absence of a frequency increase indicates that little or no energy is transferred during the first 10 ps, the duration of the oscillation; if the iodine

were to lose the 53 meV necessary for evaporation, i.e., the binding energy<sup>42</sup> of Ar to  $I_2^-$ , the oscillation frequency change would be  $\sim 5\text{ cm}^{-1}$ , which is measurable in our experiment [an increase of similar magnitude is indeed seen for  $I_2^-(Ar)_2$ , discussed in the following]. We thus conclude that no energy loss, and certainly no evaporation, occurs in  $I_2^-(Ar)$  within the first 10 ps. But the lack of rephasing at 45 ps indicates that the iodine moiety eventually interacts with the solvent, presumably causing evaporation. Thus, for this small cluster, energy loss and evaporation occurs between 10–45 ps.

The dynamics in  $I_2^-(Ar)_2$  differ from those in  $I_2^-(Ar)$ . At  $E_{\text{exc}}=0.57\text{ eV}$ , the oscillation frequency drops linearly over the 7 ps dephasing time, indicating that energy loss occurs and that there is at least one Ar atom that has not evaporated during this interval. In fact, comparison with  $I_2^-(Ar)$  suggests that *no* evaporation from  $I_2^-(Ar)_2$  occurs during the first 7 ps, since upon evaporation of an argon atom the species would become  $I_2^-(Ar)$ , which does not show evidence of energy loss prior to 10 ps at 0.57 eV, and any  $I_2^-(Ar)$  produced by evaporation of an Ar would have even less energy.

At longer times with  $E_{\text{exc}}=0.57\text{ eV}$ , the energy loss in  $I_2^-(Ar)_2$ , presuming complete solvent evaporation, is 110 meV (Table III). This would be barely enough to evaporate both argon atoms (the binding energy of an argon atom to  $I_2^-$  is  $53\text{ meV}$ <sup>42</sup>). The alternatives are either loss of  $\sim 75\text{ meV}$  with no evaporation, or loss of  $\sim 90\text{ meV}$  with evaporation of one solvent atom. In any case, the time constant  $\tau=15\text{ ps}$  indicates that at least one Ar atom remains on the cluster for  $\sim 30\text{ ps}$ , and possibly longer.

At  $E_{\text{exc}}=0.75\text{ eV}$ , at least one Ar atom remains for 4 ps, the time scale over which the oscillations increase in frequency before dephasing. No further evolution of the PE spectra occurs beyond 10 ps, suggesting that both Ar atoms may have evaporated by then. Indeed, the calculated total energy loss of 190 meV (Table III, assuming complete evaporation) would be more than enough to evaporate both argons with significant kinetic energy. An intriguing result at this energy is that the edge shift yields a more rapid drop in  $E_{\text{vib}}(\tau=1.3\text{ ps})$  than does the increase in oscillation frequency, possibly signaling rapid loss of the first argon atom, with continued energy loss and eventual evaporation of the second.

### B. $I_2^-(CO_2)$

In this small cluster,  $E_{\text{vib}}(t)$  derived from the oscillation frequency indicates that the iodine stretch loses 0.16 eV in 3.4 ps for  $E_{\text{exc}}=0.57\text{ eV}$ , and 0.28 eV in 3.8 ps for  $E_{\text{exc}}=0.75\text{ eV}$ . No evaporation is possible while the spectrum edge is still shifting or the oscillations are still increasing in frequency, so we can say that  $\sim 8\text{--}10\text{ ps}$  (about twice the edge-shift time constant  $\tau$  in Table II) is a lower bound for the time scale for evaporation, even though, particularly at the higher excitation energy, enough energy is transferred at earlier times for evaporation to occur (the  $I_2^- \cdot CO_2$  binding energy is  $230\text{ meV}$ <sup>37</sup>). This  $\sim 10\text{ ps}$  minimum time scale for evaporation is similar to that for  $I_2^-(Ar)$ , but the overall dy-

namics are quite different; in the argon cluster, no coupling between the solvent and iodine vibration appears to occur before 10 ps, while in the  $CO_2$  cluster substantial coupling and energy loss at early times do occur, but evaporation does not occur until later. The corrected values for total energy loss assuming evaporation, 230 meV for  $E_{exc}=0.57$  eV and 305 meV for  $E_{exc}=0.75$  eV (Table III), meet or exceed the  $I_2^- \cdot CO_2$  binding energy. It is likely that evaporation happens relatively soon after the spectrum stops shifting, since there are not many solvent modes in which the energy transferred from the iodine stretch may be easily stored.

This cluster apparently undergoes substantial energy loss before the first occurrence at the ITP: 70 and 135 meV for  $E_{exc}=0.57$  and 0.75 eV, respectively (Table III), a somewhat surprising result for such a small cluster. Although these values depend on our assumption of no blueshift for  $I_2^-(CO_2)$ , additional confirmation of rapid initial energy loss is provided by the observation that  $E_{vib}(t=0)$  obtained from the edge shifts (which overestimates  $E_{vib}$ ) lies below the excitation energy at 0.75 eV (see Fig. 6). For  $I_2^-(CO_2)$ , the totally symmetric cluster mode frequency was calculated to be  $59\text{ cm}^{-1}$ ,<sup>25</sup> which lies between the vibrational frequencies of  $I_2^-$  with 0.57 and 0.75 eV vibrational energy (see Table I). This near-resonance may facilitate relatively rapid coupling in  $I_2^-(CO_2)$  and probably other  $CO_2$  clusters as well, which also show evidence for rapid initial energy loss.

### C. $I_2^-(CO_2)_5$

The results for  $I_2^-(CO_2)_5$  should be directly comparable to those determined previously for  $I_2^-(CO_2)_4$ . The increased density of solvent vibrational states associated with the additional solvent molecule should result in faster energy transfer but slower evaporation, and our results allow these effects to be quantified. Figure 6 shows that by 3 ps, the  $n=5$  cluster has lost between 0.26 and 0.4 eV vibrational energy for  $E_{exc}=0.57$  eV, and between 0.4 and 0.5 eV for  $E_{exc}=0.75$  eV (the upper and lower values are from the edge shifts assuming no evaporation and the oscillation frequencies, respectively). These are similar to the values for  $I_2^-(CO_2)_4$  at  $E_{exc}=0.57$  eV, and slightly larger than the losses in the  $n=4$  cluster over the same time period for  $E_{exc}=0.75$  eV.<sup>24</sup> In each case, a large fraction of the loss by 3 ps occurs before the first ITP occurrence, at least 120 meV in 400–500 fs for the higher  $E_{exc}$  (Table III). Table II shows that the time constant  $\tau$  for the relaxation as determined by the edge shift is only slightly smaller in  $n=5$  versus  $n=4$  at  $E_{exc}=0.57$  eV, but it is significantly shorter for  $E_{exc}=0.75$  eV, 2.6 ps versus 6 ps for  $n=4$ . Overall, although the energy loss dynamics for the two clusters are similar, the  $I_2^-(CO_2)_5$  cluster exhibits somewhat faster and greater energy loss from the  $I_2^-$  chromophore than the  $n=4$  cluster, especially at the higher excitation energy.

Both clusters show enough energy loss within the first several picoseconds such that evaporation of the maximum number of solvent molecules as found in the reflectron studies<sup>37</sup> could occur, as per the larger long-time loss values in Table III. But we cannot determine the time scale for evaporation for either cluster from our data. Simulations<sup>12</sup> of

FPE spectra from the photodissociation of  $I_2^-(CO_2)_n$  indicate that the final evaporation of solvent molecules from the vibrationally relaxing recombined  $I_2^-$  may take hundreds of picoseconds, but such studies were done with much higher excess energy and more solvent molecules than in the current SEP studies. In any event, the solvent network in  $I_2^-(CO_2)_5$  should have a much greater capacity to store the energy released from the iodine than any of the other clusters studied here.

### D. $I_2^-(Ar)_6$ and $I_2^-(Ar)_9$

These clusters exhibit intermediate dynamics, generally showing less total energy loss than the  $n=4,5$   $CO_2$  clusters, but more than the smaller clusters. At short times, before dephasing of the oscillations occurs, the dynamics of  $I_2^-(Ar)_6$  and  $I_2^-(Ar)_9$  at each excitation energy are quite similar, both in terms of initial energy loss (Table III) and relaxation rate as determined by the frequency shift (Table I). At each energy, the relaxation rate for the  $n=9$  cluster is only slightly larger than that for the  $n=6$  cluster, but the relaxation rates for both clusters are significantly higher at 0.75 eV than at 0.57 eV. The overall relaxation time constants as determined from the edge shifts are again quite similar at 0.57 eV (from Table II,  $\tau=28$  ps for both clusters). At 0.75 eV, both time constants decrease, but the change for the  $n=6$  cluster, to  $\tau=6.4$  ps, is considerably more precipitous than for the  $n=9$  cluster ( $\tau=16.4$  ps). These distinctions can be seen more clearly in Figs. 4 and 7. At 0.75 eV, the  $I_2^-(Ar)_6$  edge shifts and the associated value of  $E_{vib}(t)$  flatten out abruptly beyond 10 ps, whereas the plots for  $I_2^-(Ar)_6$  at 0.57 eV and  $I_2^-(Ar)_9$  at both energies continue to evolve out to 150 ps, the maximum time plotted in the figures.

The interplay of relaxation and evaporation is of particular interest in these clusters, as far as determining which process is responsible for the observed dynamics over a particular time interval. One might expect that at a given excitation energy, relaxation is faster for the larger cluster because of the higher density of vibrational states, and that evaporation should be slower for the same reason. The values of  $E_{vib}(t)$  at short times derived from the oscillation frequency indeed drop more rapidly for the  $n=9$  at each excitation energy (Table I, Fig. 6), as expected from these considerations. The edge shifts, however, depend on both relaxation and evaporation dynamics, and the time constants  $\tau$  reflect this, being essentially the same for the two clusters at 0.57 eV and noticeably larger for the  $n=9$  cluster at 0.75 eV. More specifically, the results for these two clusters plotted in Figs. 4 and 7 imply that evaporation is largely complete by 10 ps for  $I_2^-(Ar)_6$  at 0.75 eV, beyond which little evolution of the PE spectra is seen, but the other three data sets imply that relaxation and solvent evaporation are still occurring at least out to 100 ps. If our interpretation of the edge shifts for  $I_2^-(Ar)_6$  at 0.75 eV is correct, then it is almost certain that some solvent evaporation is occurring over the time scale that oscillations are observed for this cluster (3–4 ps), implying that coherent motion of the  $I_2^-$  core can be observed concurrently with solvent evaporation, and providing the strongest evidence yet that vibrational relaxation and

evaporation occur on similar time scales in  $I_2^-(Ar)_n$  clusters. This view is consistent with the FPE and simulation results of photodissociation of large  $I_2^-(Ar)_n$  clusters,<sup>11,16</sup> discussed in Sec. I. It is substantiated as well by the long-time energy losses displayed in Table III, the larger values of which correspond almost exactly to the energy needed to evaporate all of the  $n$  (6 or 9) solvent atoms.

## VI. CONCLUSIONS

We have carried out experiments in which a known amount of energy is initially deposited into the iodine stretch of an  $I_2^-(S)_n$  cluster via femtosecond stimulated emission pumping. We use time-resolved photoelectron spectroscopy as a means of monitoring the subsequent vibrational relaxation as the iodine loses energy to the cluster modes. We have investigated several cluster sizes with two solvent species, Ar and CO<sub>2</sub>, at excitation energies of 0.57 and 0.75 eV. As in our previous fs-SEP publication, which focused on  $I_2^-(CO_2)_4$ ,<sup>24</sup> we determine how much energy remains in the  $I_2^-$  stretch [ $E_{\text{vib}}(t)$ ] using either of two methods: by analyzing the oscillation frequency of the vibrationally excited ground state wave packet as measured at the inner turning point, and by converting the high-kinetic-energy edge of the spectrum directly to vibrational energy. These methods provide lower and upper bounds, respectively, for  $E_{\text{vib}}(t)$ , but the value derived from the oscillation frequency should be quite accurate for several of the smaller clusters. All clusters but  $I_2^-(Ar)$  show evidence for rapid energy loss during the first half-oscillation of the wave packet in the potential.

Vibrational energy loss is significantly faster in  $I_2^-(CO_2)_n$  clusters than in  $I_2^-(Ar)_n$  clusters, a result that can be understood in terms of stronger chromophore-solvent coupling and higher densities of solvent intermolecular vibrational states in  $I_2^-(CO_2)_n$  clusters. Solvation effects are minimal for  $I_2^-(Ar)$ , where the oscillation frequency is essentially identical to that of the bare solute, and the only evidence for interaction is the absence of rephasing near 45 ps. Addition of a second argon atom speeds up the process significantly.  $I_2^-(CO_2)$  shows much greater and faster energy loss than  $I_2^-(Ar)$ ; the minimum time scale for evaporation of the single solvent is similar, however. In larger  $I_2^-(CO_2)_n$  ( $n=4,5$ ) clusters, the time scales for relaxation are similar ( $\sim 3-6$  ps) at both excitation energies, though addition of a fifth CO<sub>2</sub> molecule lowers the overall time scale slightly. In larger  $I_2^-(Ar)_n$  ( $n=6,9$ ) clusters, in contrast, the time scale depends strongly on the number of solvent atoms and on the excitation energy, with the smaller cluster at higher energy having the fastest time scale for energy transfer. We believe that the differences between  $I_2^-(Ar)_{6,9}$  and  $I_2^-(CO_2)_{4,5}$  are caused by the differing roles played by solvent evaporation; argon atoms evaporate in close correlation with vibrational energy loss, while the CO<sub>2</sub> solvent network stores energy for longer periods of time before evaporation occurs.

Future work in our laboratory will utilize our new photoelectron imaging detector,<sup>45</sup> which allows the determination of the photoelectron angular distributions as well as their kinetic energies, and has a much better resolution than the

current time-of-flight detector. This may be useful in future fs-SEP studies by making possible the separation of vibrationally excited wave packet dynamics from the residual upper-state intensity, especially near the outer turning point region of the spectrum, which is too congested to examine currently. Additionally, the interpretation of the current work, particularly the role of evaporation, would be greatly aided by molecular dynamics simulations of vibrationally excited  $I_2^-$  within a solvent cluster.

## ACKNOWLEDGMENTS

This research is supported by the National Science Foundation under Grant No. CHE-0092574. R.W. acknowledges support from the Alexander von Humboldt-Stiftung and from the Emmy Noether-Program of the Deutsche Forschungsgemeinschaft. A.E.B. is a National Science Foundation predoctoral fellow.

- <sup>1</sup>M. A. Duncan, *Int. J. Mass. Spectrom.* **200**, 545 (2000).
- <sup>2</sup>R. Parson, J. Faeder, and N. Delaney, *J. Phys. Chem. A* **104**, 9653 (2000).
- <sup>3</sup>A. Sanov and W. C. Lineberger, *PhysChemComm* **5**, 165 (2002).
- <sup>4</sup>P. K. Walhout, J. C. Alfano, K. A. M. Thakur, and P. F. Barbara, *J. Phys. Chem.* **99**, 7568 (1995).
- <sup>5</sup>V. Vorsa, P. J. Campagnola, S. Nandi, M. Larsson, and W. C. Lineberger, *J. Chem. Phys.* **105**, 2298 (1996).
- <sup>6</sup>J. M. Papanikolas, V. Vorsa, M. E. Nadal, P. J. Campagnola, H. K. Buchenau, and W. C. Lineberger, *J. Chem. Phys.* **99**, 8733 (1993).
- <sup>7</sup>V. Vorsa, S. Nandi, P. J. Campagnola, M. Larsson, and W. C. Lineberger, *J. Chem. Phys.* **106**, 1402 (1997).
- <sup>8</sup>J. M. Papanikolas, J. R. Gord, N. E. Levinger, D. Ray, V. Vorsa, and W. C. Lineberger, *J. Phys. Chem.* **95**, 8028 (1991).
- <sup>9</sup>B. J. Greenblatt, M. T. Zanni, and D. M. Neumark, *Science* **276**, 1675 (1997).
- <sup>10</sup>B. J. Greenblatt, M. T. Zanni, and D. M. Neumark, *Faraday Discuss.* **108**, 101 (1998).
- <sup>11</sup>B. J. Greenblatt, M. T. Zanni, and D. M. Neumark, *J. Chem. Phys.* **111**, 10566 (1999).
- <sup>12</sup>B. J. Greenblatt, M. T. Zanni, and D. M. Neumark, *J. Chem. Phys.* **112**, 601 (2000).
- <sup>13</sup>J. M. Papanikolas, P. E. Maslen, and R. Parson, *J. Chem. Phys.* **102**, 2452 (1995).
- <sup>14</sup>J. Faeder, N. Delaney, P. E. Maslen, and R. Parson, *Chem. Phys. Lett.* **270**, 196 (1997).
- <sup>15</sup>N. Delaney, J. Faeder, P. E. Maslen, and R. Parson, *J. Phys. Chem. A* **101**, 8148 (1997).
- <sup>16</sup>J. Faeder and R. Parson, *J. Chem. Phys.* **108**, 3909 (1998).
- <sup>17</sup>J. Faeder, N. Delaney, P. E. Maslen, and R. Parson, *Chem. Phys.* **239**, 525 (1998).
- <sup>18</sup>N. Delaney, J. Faeder, and R. Parson, *J. Chem. Phys.* **111**, 452 (1999).
- <sup>19</sup>V. S. Batista and D. F. Coker, *J. Chem. Phys.* **110**, 6583 (1999).
- <sup>20</sup>V. S. Batista and D. F. Coker, *J. Chem. Phys.* **106**, 7102 (1997).
- <sup>21</sup>C. J. Margulis and D. F. Coker, *J. Chem. Phys.* **110**, 5677 (1999).
- <sup>22</sup>E. Cho and S. Shin, *J. Chem. Phys.* **117**, 6047 (2002).
- <sup>23</sup>A. V. Davis, M. T. Zanni, C. Frischkorn, M. Elhanine, and D. M. Neumark, *J. Electron Spectrosc. Relat. Phenom.* **112**, 221 (2000).
- <sup>24</sup>A. V. Davis, R. Wester, A. E. Bragg, and D. M. Neumark, *J. Chem. Phys.* **117**, 4282 (2002).
- <sup>25</sup>H. Gómez, T. R. Taylor, and D. M. Neumark, *J. Chem. Phys.* **116**, 6111 (2002).
- <sup>26</sup>M. T. Zanni, Ph.D. thesis, University of California, Berkeley, 1999.
- <sup>27</sup>R. Pausch, M. Heid, T. Chen, W. Kiefer, and H. Schwoerer, *J. Chem. Phys.* **110**, 9560 (1999).
- <sup>28</sup>G. Knopp, I. Pinkas, and Y. Prior, *J. Raman Spectrosc.* **31**, 51 (2000).
- <sup>29</sup>I. Pinkas, G. Knopp, and Y. Prior, *J. Chem. Phys.* **115**, 236 (2001).
- <sup>30</sup>A. E. Johnson, N. E. Levinger, and P. F. Barbara, *J. Phys. Chem.* **96**, 7841 (1992).
- <sup>31</sup>D. A. V. Kliner, J. C. Alfano, and P. F. Barbara, *J. Chem. Phys.* **98**, 5375 (1993).

- <sup>32</sup>J. C. Alfano, Y. Kimura, P. K. Walhout, and P. F. Barbara, *Chem. Phys.* **175**, 147 (1993).
- <sup>33</sup>U. Banin and S. Ruhman, *J. Chem. Phys.* **99**, 9318 (1993).
- <sup>34</sup>U. Banin, A. Waldman, and S. Ruhman, *J. Chem. Phys.* **96**, 2416 (1992).
- <sup>35</sup>I. Benjamin, U. Banin, and S. Ruhman, *J. Chem. Phys.* **98**, 8337 (1993).
- <sup>36</sup>I. Benjamin, P. F. Barbara, B. J. Gertner, and J. T. Hynes, *J. Phys. Chem.* **99**, 7557 (1995).
- <sup>37</sup>R. Wester, A. V. Davis, A. E. Bragg, and D. M. Neumark, *Phys. Rev. A* **65**, 051201 (2002).
- <sup>38</sup>M. T. Zanni, A. V. Davis, C. Frischkorn, M. Elhanine, and D. M. Neumark, *J. Chem. Phys.* **112**, 8847 (2000).
- <sup>39</sup>R. J. LeRoy, *J. Chem. Phys.* **52**, 2683 (1970).
- <sup>40</sup>S. Gerstenkorn and P. Luc, *J. Phys. (France)* **46**, 867 (1985).
- <sup>41</sup>F. Martin, R. Bacis, S. Churassy, and J. Verges, *J. Mol. Spectrosc.* **116**, 71 (1986).
- <sup>42</sup>K. R. Asmis, T. R. Taylor, C. Xu, and D. M. Neumark, *J. Chem. Phys.* **109**, 4389 (1998).
- <sup>43</sup>M. T. Zanni, B. J. Greenblatt, and D. M. Neumark, *J. Chem. Phys.* **109**, 9648 (1998).
- <sup>44</sup>H. Hotop and W. C. Lineberger, *J. Phys. Chem. Ref. Data* **14**, 731 (1985).
- <sup>45</sup>A. V. Davis, R. Wester, A. E. Bragg, and D. M. Neumark, *J. Chem. Phys.* **118**, 999 (2003).